Nuclear Uptake and Dosimetry of ^{64}Cu-Labeled Chelator–Somatostatin Conjugates in an SSTr2-Transfected Human Tumor Cell Line

Martin Eiblmaier[1], Rebecca Andrews[2], Richard Laforest[1], Buck E. Rogers[2], and Carolyn J. Anderson[1]

[1]*Mallinckrodt Institute of Radiology, Washington University School of Medicine, Saint Louis, Missouri; and* [2]*Department of Radiation Oncology, Washington University School of Medicine, Saint Louis, Missouri*

^{64}Cu radiopharmaceuticals have shown tumor growth inhibition in tumor-bearing animal models with a relatively low radiation dose that may be related to nuclear localization of the ^{64}Cu in tumor cells. Here we address whether the nuclear localization of ^{64}Cu from a ^{64}Cu-labeled chelator–somatostatin conjugate is related to the dissociation of the radio-copper from its chelator. The ^{64}Cu complex of 1,4,8,11-tetraazacyclotetradecane-1,4,8,11-tetraacetic acid (TETA) has demonstrated instability in vivo, whereas ^{64}Cu-CB-TE2A (CB-TE2A is 4,11-bis(carboxymethyl)-1,4,8,11-tetraazabicyclo[6.6.2]hexadecane) was highly stable. **Methods:** Receptor binding, nuclear uptake, internalization, and efflux assays were performed to characterize the interaction with the somatostatin receptor and the intracellular fate of ^{64}Cu-labeled chelator–peptide conjugates in A427-7 cells. From these data, the absorbed dose to cells was calculated. **Results:** ^{64}Cu-TETA-Y3-TATE (^{64}Cu-**[1]**) and ^{64}Cu-CB-TE2A-Y3-TATE (^{64}Cu-**[2]**) had high affinity for somatostatin receptor subtype 2 (SSTr2) in A427-7 cells. After 3 h, ^{64}Cu-**[2]** showed greater internalization (>30%) compared with ^{64}Cu-**[1]** (~15%). There was uptake of ^{64}Cu-**[1]** in nuclei of 427–7 cells (9.4% ± 1.7% at 24 h), whereas ^{64}Cu-**[2]** showed minimal nuclear accumulation out to 24 h (1.3% ± 0.1%). A427-7 cells were exposed to 0.40 Gy from ^{64}Cu-**[1]** and exposed to 1.06 Gy from ^{64}Cu-**[2]**. External beam irradiation of A427-7 cells showed <20% cell killing at 1 Gy. **Conclusion:** These results are consistent with our hypothesis that dissociation of ^{64}Cu from TETA leads to nuclear localization. Dosimetry calculations indicated that the nuclear localization of ^{64}Cu-**[1]** was not significant enough to increase the absorbed dose to the nuclei of A427-7 cells. These studies show that ^{64}Cu localization to cell nuclei from internalizing, receptor-targeted radiopharmaceuticals is related to chelate stability.

Key Words: ^{64}Cu; targeted radiotherapy; somatostatin receptor; somatostatin analog; dosimetry

J Nucl Med 2007; 48:1390–1396
DOI: 10.2967/jnumed.107.039990

Radiolabeled somatostatin analogs have become important agents for molecular imaging and targeted radiotherapy of somatostatin-receptor (SSTr)–positive tumors. Gamma scintigraphy with ^{111}In-diethylenetriaminepentaacetic acid-octreotide (^{111}In-DTPA-octreotide; OctreoScan, Mallinckrodt) has become the standard method to image neuroendocrine tumors (*1,2*) and is clinically approved in Europe and the United States. Somatostatin analogs labeled with ^{111}In, ^{90}Y, ^{177}Lu, and ^{64}Cu have been evaluated for targeted radiotherapy of cancer in animal models (*3–7*), and clinical trials have been performed with ^{90}Y-1,4,7,10-tetraazacyclododecane-1,4,7,10-tetraacetic acid tyrosine^3-octreotide (^{90}Y-DOTATOC) and ^{177}Lu-DOTA-tyrosine^3-octreotate (^{177}Lu-DOTATATE) in patients with neuroendocrine tumors with promising results (*8–11*).

^{64}Cu (half-life = 12.7 h; β^+ [17.4%]; β^- [41%]) emits both β^+ and β^- radiation, allowing for the use of this radionuclide in both PET and targeted radiotherapy of cancer. Thus, ^{64}Cu-labeled somatostatin analogs have the potential as dual-use agents for imaging and radionuclide therapy, reinforcing the arsenal of radiopharmaceuticals (*12*) available to treat SSTr–positive tumors. We previously observed that ^{64}Cu-labeled tumor-targeting agents showed enhanced therapeutic efficacy of an internalizing ^{64}Cu-labeled anticolorectal carcinoma monoclonal antibody (mAb), ^{64}Cu-labeled 1A3, in a tumor-bearing rodent model compared with ^{90}Y- or ^{131}I-labeled mAbs in the same animal model (*13,14*). We also evaluated the ^{64}Cu-labeled somatostatin analogs octreotide and tyrosine^3-octreotate (Y3-TATE) as therapeutic agents. Although we did not observe complete tumor remissions, we did see tumor growth inhibition at relatively low radiation doses to the tumors (465–600 cGy) (*6,7*).

We previously demonstrated that ^{64}Cu from ^{64}Cu-1,4,8,11-tetraazacyclotetradecane-1,4,8,11-tetraacetic acid-octreotide (^{64}Cu-TETA-octreotide) was significantly localized in the nuclei of AR42J rat pancreatic tumor cells in cell culture, whereas ^{111}In from ^{111}In-DTPA-octreotide was found in the tumor cell nuclei in only very small amounts (*15*). These

Received Jan. 19, 2007; revision accepted May 15, 2007.
For correspondence or reprints contact: Carolyn J. Anderson, PhD, Mallinckrodt Institute of Radiology, Washington University School of Medicine, 510 S. Kingshighway Blvd., Campus Box 8225, St. Louis, MO 63130.
E-mail: andersoncj@wustl.edu

data suggested that delivery of ^{64}Cu to the cell nuclei may enhance the therapeutic effect of β-emitting, tumor-targeting copper radiopharmaceuticals. In this study, the effect of the Cu(II) chelator on the delivery of ^{64}Cu to tumor cell nuclei was evaluated to study the intracellular fate of the radiometal in somatostatin analogs, and the potential consequences on cell survival. ^{64}Cu-1,4,8,11-tetraazacyclotetradecane-1,4,8,11-tetraacetic acid tyrosine^3-octreotate (^{64}Cu-TETA-Y3-TATE) and ^{64}Cu-4,11-bis(carboxymethyl)-1,4,8,11-tetraazabicyclo [6.6.2]hexadecane-tyrosine^3-octreotate (^{64}Cu-CB-TE2A-Y3-TATE) were evaluated in the highly expressing, somatostatin receptor subtype 2 (SSTr2) transfected A427-7 human non–small cell lung cancer cell line (*16*). We hypothesized that ^{64}Cu from ^{64}Cu-TETA-Y3-TATE, but not from ^{64}Cu-CB-TE2A-Y3-TATE, would dissociate from the complex after internalization by the SSTr2 and localize to the cell nucleus. Here we compared the nuclear localization of ^{64}Cu from ^{64}Cu-TETA-Y3-TATE with that of the more stable ^{64}Cu-CB-TE2A-Y3-TATE and determined the absorbed radiation dose to A427-7 cells grown in cell culture.

MATERIALS AND METHODS

Materials

1,4,8,11-Tetraazacyclotetradecane-1,4,8,11-tetraacetic acid (TETA) was obtained from Macrocyclics, and 4,11-bis(carboxymethyl)-1,4,8,11-tetraazabicyclo[6.6.2]hexadecane (CB-TE2A) was provided by Gary Weisman from the University of New Hampshire (*17*). Y3-TATE was synthesized and conjugated to TETA and CB-TE2A by CSBio using previously published methods (*17*). All reagents for receptor-binding assays were purchased from Sigma-Aldrich.

The stable transfection of A427 non–small lung cancer cells with *SSTr2* has been described elsewhere (*16*). A427-7 cell medium (minimum essential Eagle medium in Earle's balanced salt solution) was obtained from Gibco and supplemented with 1 mM nonessential amino acids (Sigma-Aldrich), 10 mM sodium pyruvate (Sigma-Aldrich), and 10% fetal bovine serum (Gibco).

Radiochemistry

TETA-Y3-TATE **[1]** (1 μg) was labeled with 19–74 MBq (0.5–2 mCi) of [^{64}Cu]cupric acetate by incubation in 100–150 μL of 0.1 M ammonium acetate (pH 5.5) for 1 h at room temperature (RT) as previously described to yield ^{64}Cu-TETA-Y3-TATE (^{64}Cu**-[1]**) (*7*). ^{64}Cu-CB-TE2A-Y3-TATE (^{64}Cu**-[2]**) was produced by incubating 1 μg of CB-TE2A-Y3-TATE **[2]** with 9–37 MBq (0.25–1 mCi) of [^{64}Cu]cupric acetate in 100–150 μL of 0.1 M ammonium acetate (pH 8.0) for 1.5 h at 95°C as previously described (*17*). Radiochemical purity was confirmed by radio-thin layer chromatography (radio-TLC) (C18 plate; mobile phase, 10% ammonium acetate:methanol = 3:7). $^{nat}CuCl_2$ was used to synthesize ^{nat}Cu**-[1]** and ^{nat}Cu**-[2]** from **[1]** and **[2]** under identical conditions.

Receptor-Binding Assays

A427-7 cell membrane preparations for binding assays were prepared as previously described (*16*). Assays were performed on a 96-well Multiscreen Durapore filtration plate (Millipore) using methods previously described with some modifications (*17*). Membranes were diluted in binding buffer (50 mM Tris-HCl, pH 7.4, 5 mM $MgCl_2 \cdot 6\ H_2O$, 0.1% bovine serum albumin [BSA], 0.5 μg/mL aprotinin, 200 μg/mL bacitracin, 10 μg/mL leupeptin, and 10 μg/mL pepstatin A), and 5–30 μg of membrane protein were used per well. In competitive binding assays, ^{64}Cu-**[1]** or ^{64}Cu-**[2]** were displaced with increasing concentrations (0.01 nM–1 μM) of ^{nat}Cu-**[1]** or ^{nat}Cu-**[2]**, respectively. In saturation binding assays, increasing concentrations (0.05–15 nM) of ^{64}Cu-**[1]** or ^{64}Cu-**[2]** were added to membranes to measure total binding, and nonspecific binding was determined by conducting the assay in the presence of an excess (200 nM) of **[1]** or **[2]**. After incubation at RT for 2 h, the medium was removed with a vacuum manifold, and the membranes were washed twice with 200 μL binding buffer. OptiPhase Super-Mix (Perkin Elmer) (25 μL) was added to each well, and bound activity was measured with a 1450 Microbeta liquid scintillation and luminescence counter (Perkin Elmer). In competitive binding assays, 50% inhibitory concentration (IC_{50}) values were estimated from nonlinear curve fitting of bound peptide versus the sum of the concentrations of ^{64}Cu- and ^{nat}Cu-labeled peptide using Prism (GraphPad) software. In saturation binding assays, specific binding was obtained by subtraction of nonspecific binding from total binding. Maximum binding capacities (B_{max}) were estimated from nonlinear curve fitting of specific binding versus the concentration of ^{64}Cu-labeled peptide using Prism.

Nuclear Localization

^{64}Cu-**[1]** or ^{64}Cu-**[2]** was added to A427-7 cells in T-175 culture flasks (~10^7 cells/flask, ligand:receptor = 1:10 based on the respective B_{max}). Cells were incubated at 37°C for various time periods, after which the medium was removed, cells were washed carefully with phosphate-buffered saline (PBS) and were removed from the flask with a cell scraper tool. A427-7 nuclei were isolated as described previously (*15*). ^{64}Cu activity in the nuclear fraction, the lysate supernatant, and the medium was measured with a Beckman 8000 automated well-type gamma counter. The percentage in the nucleus was determined by the gamma counts in the pure nuclei divided by the gamma counts associated with whole cells. Aliquots of nuclei were assayed qualitatively for purity by fluorescence microscopy after staining with fluorescein isothiocyanate ([FITC] 3 μg/mL) and propidium iodide (7 μg/mL) as described previously (*15*).

Internalization and Efflux Profiles

^{64}Cu-**[1]** or ^{64}Cu-**[2]** (5–50 pmol) was added to A427-7 cells cultured at 37°C in 6-well plates (~$5 \cdot 10^5$ cells/well). Internalization during a pulse of 4 h and efflux of the radioactivity during the 20 h after the pulse were monitored. At various time points, the medium was aspirated and the cells were washed twice with 1 mL Hanks' buffered salt solution (HBSS) and incubated for 10 min at 37°C in 1 mL HBSS supplemented with 20 mM sodium acetate (pH 4.0) to remove peptide bound to the cell surface. The cells were lysed by incubation with 0.5% sodium dodecyl sulfate in PBS (80°C, 30 min). ^{64}Cu activities in the medium, the cell-surface wash, and the cell lysate were measured with a gamma counter.

External Beam Irradiation

A427-7 cells were plated in T25 flasks and 24 h later were irradiated at 0, 2, 4, 6, 8, and 10 Gy using a PANTAK pmc1000 x-ray machine at a dose rate of ~0.9 cGy/min. The cells were immediately trypsinized and counted, and different cell numbers were seeded on p60 plates in triplicate. The cells were grown for 12 d to allow for colony formation and then fixed with ethanol and

stained with crystal violet. Colonies (>50 cells) were counted and the data were normalized to the cells that were not irradiated.

Dosimetry

Internalization/efflux data were replotted in disintegrations per second per cell (dps/cell), and disintegrations per cell over the course of the experiment were calculated from the area-under-curve function of GraphPad Prism. To the total number of disintegrations was added the number of disintegrations past the last time point (24 h) assuming only physical decay (no biologic washout from the cell surface or nucleus). The absorbed dose to whole cells and to the nuclei was calculated from the total number of decays by a linear combination of S values and disintegration numbers (using cellular S values for ^{64}Cu, and a cell radius of 10 μm and a nuclear radius of 9 μm) (*18*). MIRD methodology for cellular dosimetry considers either the whole cell as the source organ or the cell surface, the cytoplasm, and the nucleus. In this experiment, the cytoplasm activity was provided by the difference between the measured internalized activity and the activity assigned to the nucleus. The total absorbed dose to the cell nucleus is provided by:

$$D_N = A_{Cy}S(N \leftarrow Cy) + A_{CS}S(N \leftarrow CS) + A_NS(N \leftarrow N),$$

and the absorbed radiation dose to the whole cell is:

$$D_C = A_{CS}S(C \leftarrow CS) + A_CS(C \leftarrow C),$$

where A_{Cy}, A_C, A_{CS}, and A_N are the total number of disintegrations in the cytoplasm, in the whole cell, at the cell surface, and in the nucleus. The S(target organ ← source organ) are the cellular S values in Gy/Bq·s. These calculations were made with the assumption that the absorbed dose from decay occurring in a neighboring cell does not contribute to the total dose of a given cell. This assumption is justified here as the experiment was performed in a single-layer cell culture and the distance is relatively large.

RESULTS

Radiochemistry

Radiolabeling of TETA-Y3-TATE **[1]** and CB-TE2A-Y3-TATE **[2]** with ^{64}Cu produced ^{64}Cu-TETA-Y3-TATE (^{64}Cu-**[1]**) and ^{64}Cu-CB-TE2A-Y3-TATE (^{64}Cu-**[2]**) with ≥95% radiochemical purity as determined by radio-TLC. The R_f values for these compounds were significantly different (0.79 ± 0.01, n = 6, for ^{64}Cu-**[1]**; 0.63 ± 0.01, n = 7, for ^{64}Cu-**[2]**; $P < 0.0001$).

Receptor Binding

Competitive and saturation receptor-binding assays were performed to examine the interaction of both somatostatin analogs with SSTr2 on transfected A427-7 cells. Assays were conducted using isolated A427-7 cell membranes with a defined amount of membrane protein (5–30 μg/well). In competitive receptor-binding experiments, ^{64}Cu-**[1]** (0.070 nM) and ^{64}Cu-**[2]** (0.057 nM) were displaced from A427-7 membranes by increasing concentrations of ^{nat}Cu-**[1]** and ^{nat}Cu-**[2],** respectively. The IC_{50} values for both compounds were not significantly different: 4.87 ± 1.11 nM for ^{64}Cu-**[1]** and 3.71 ± 1.09 nM for ^{64}Cu-**[2]**.

The binding constants (K_d) were not significantly different (0.22 ± 0.02 nM, n = 3, for ^{64}Cu-**[1]**; 0.61 ± 0.24 nM, n = 3, for ^{64}Cu-**[2]**; P = 0.18) and were found to be in the expected range for somatostatin analogs (*17*). Even though the maximum binding capacities (B_{max}) were not statistically significantly different (5,440 ± 1,110 fmol/mg, n = 3, for ^{64}Cu-**[1]**; 11,400 ± 1,960 fmol/mg, n = 3, for ^{64}Cu-**[2]**; P = 0.06), there was a clear tendency to higher values for ^{64}Cu-**[2]**. This phenomenon has been observed previously with AR42J cells for these 2 compounds (*17*). Plots of the competitive and representative saturation binding experiments are shown in Figure 1, and Table 1 summarizes the receptor-binding parameters for both compounds.

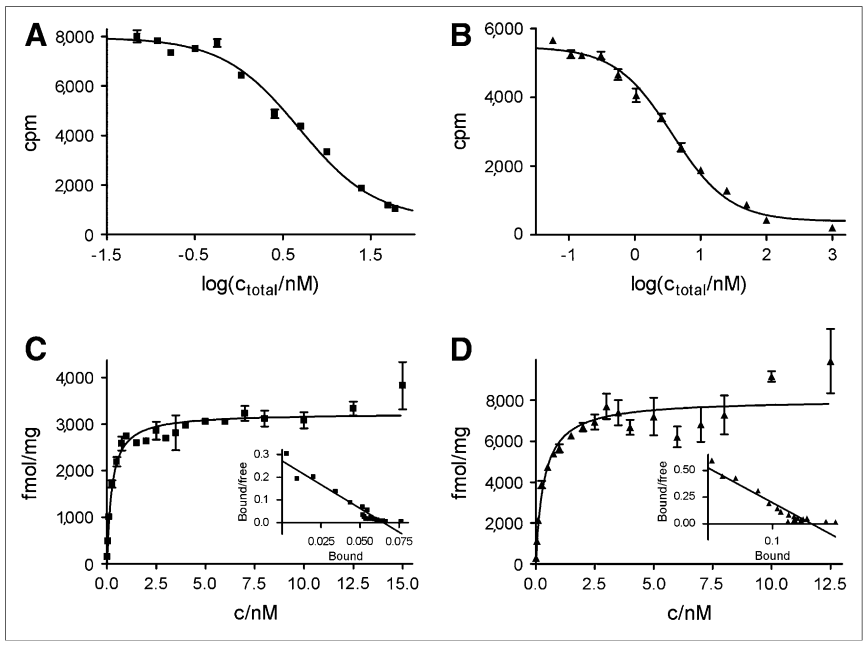

FIGURE 1. Receptor binding of ^{64}Cu-TETA-Y3-TATE (■: IC_{50} = 4.87 ± 1.11 nM, K_d = 0.22 ± 0.02 nM, B_{max} = 5,440 ± 1,110 fmol/mg) and ^{64}Cu-CB-TE2A-Y3-TATE (▲: IC_{50} = 3.71 ± 1.09 nM, K_d = 0.61 ± 0.24 nM, B_{max} = 11,400 ± 1,960 fmol/mg) to A427-7 cell membranes. (A) and (B) Competitive receptor binding. (C) and (D) Representative saturation binding experiments. Insets: Scatchard plots.

TABLE 1
Receptor-Binding Parameters for 2 Somatostatin Analogs and SSTr2 of A427-7 Human Non–Small Cell Lung Carcinoma Cells

Somatostatin analog	IC_{50} (nM)	K_d (nM)	B_{max} (fmol/mg)
^{64}Cu-TETA-Y3-TATE	4.87 ± 1.11	0.22 ± 0.02	5,440 ± 1,110
^{64}Cu-CB-TE2A-Y3-TATE	3.71 ± 1.09	0.61 ± 0.24	11,400 ± 1,960

Nuclear Localization of ^{64}Cu from [1] and [2] in A427-7 Nuclei

A427-7 cells were continuously incubated with ^{64}Cu-**[1]** or ^{64}Cu-**[2]**. ^{64}Cu activity in the media, whole cells, cell lysates, and cell nuclei was measured at various time points. Figure 2 depicts the localization of ^{64}Cu from ^{64}Cu-**[1]** and ^{64}Cu-**[2]** in A427-7 nuclei. The rate of internalization differed substantially for the 2 compounds (data not shown) (*17*), with ^{64}Cu-**[2]** entering the cells faster than ^{64}Cu-**[1]**. To correct for this increased uptake of ^{64}Cu-**[2]**, the data are plotted as the percentage of cell-associated activity (% CAA) rather than the percentage initial dose (%ID). Whereas incubation with ^{64}Cu-**[2]** did not lead to accumulation of ^{64}Cu in the nuclear fraction (1.3% ± 0.1% CAA at 24 h), there was considerable uptake of ^{64}Cu-**[1]** in the nuclei of A427-7 cells (9.4% ± 1.7% CAA at 24 h). This nuclear uptake was low initially and increased substantially after the first 12 h of the experiment. These results are consistent with our hypothesis of dissociation of ^{64}Cu from the TETA chelator in ^{64}Cu-**[1]**, but not from CB-TE2A in ^{64}Cu-**[2]**, before ^{64}Cu trafficking to the cell nucleus.

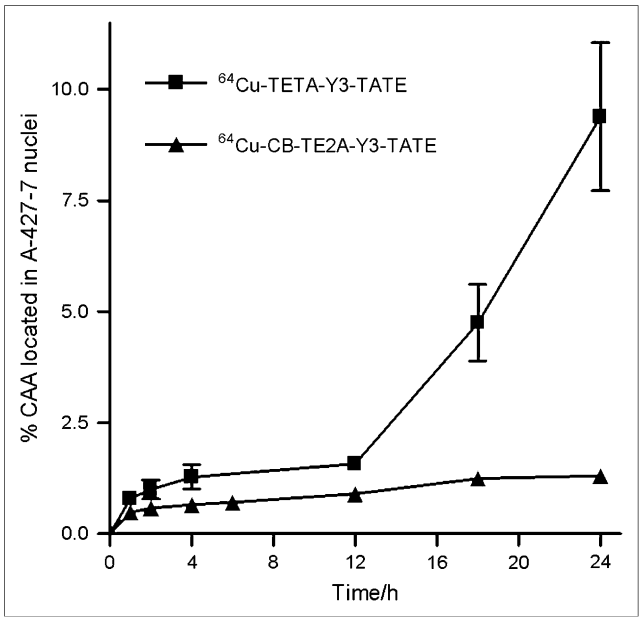

FIGURE 2. Nuclear uptake of ^{64}Cu-TETA-Y3-TATE (■) and ^{64}Cu-CB-TE2A-Y3-TATE (▲) shown as percentage of cell-associated activity (% CAA) located in A427-7 nuclei (n = 2–4 for 1-, 2-, 4-, 6-, and 12-h time points; n = 5 for 18-h time point; n = 6 for 24-h time point).

Samples of isolated nuclei were treated with FITC, which stains protein, and propidium iodide, which stains nucleic acids, to confirm purity. As previously demonstrated (*15*), no visible cellular debris was detected in the nuclear fractions (data not shown).

Internalization and Efflux Profiles

A427-7 cells were incubated with 50 pmol (5.44 kBq/pmol [0.147 μCi/pmol]) of ^{64}Cu-**[1]** or ^{64}Cu-**[2]**. After 4 h, the radiopharmaceutical-containing medium was replaced with fresh medium, and cells were incubated for an additional 20 h. Profiles for the activity internalized into cells and bound to the cell surface are shown in Figure 3A. The amount of ^{64}Cu-**[2]** bound to the surface of A427-7 cells exceeds the amount of surface-bound ^{64}Cu-**[1]** at all time points. This finding is consistent with the higher B_{max} measured for ^{64}Cu-**[2]**. As in the nuclear uptake experiments, substantially more ^{64}Cu-**[2]** than ^{64}Cu-**[1]** is internalized into A427-7 cells. For both compounds, the amount of internalized activity peaks at 3 h, when the cells' capacity for uptake ends. The decrease in activity after the change to fresh medium is primarily due to the radioactive decay of ^{64}Cu, and not to efflux of either ^{64}Cu-**[1]** or ^{64}Cu-**[2]**, which can be seen by replotting the data as %ID over time (Fig. 3B).

Dosimetry

Internalization/efflux data were replotted in dps/cell to calculate the disintegrations per cell over the course of the experiment, by using the area-under-curve function of GraphPad Prism. Cell numbers were calculated from protein mass as determined by a bicinchoninic acid (BCA) protein assay (Pierce). Several control experiments confirmed that there are ~$1.9 \cdot 10^6$ cells/mg protein for A427-7 cells (data not shown). Nuclear uptake data were used to estimate the percentage of internalized activity that translocated to A427-7 nuclei. Figure 3C displays ^{64}Cu activities in A427-7 nuclei from ^{64}Cu-**[1]** and ^{64}Cu-**[2]**. Despite ^{64}Cu-**[2]** being more efficiently internalized, the amount of ^{64}Cu from ^{64}Cu-**[1]** entering the cell nucleus is similar to that of ^{64}Cu-**[2]** at early time points and higher at later time points. Disintegrations per cell were used to calculate the absorbed dose to the whole cell and to the cell nucleus: A427-7 cells were exposed to 0.40 Gy in the case of ^{64}Cu-**[1]**, 0.15 Gy of which can be partitioned to A427-7 cell nuclei. With ^{64}Cu-**[2]**, the respective values were 1.06 Gy and 0.38 Gy (Fig. 4A). The nuclear dose from ^{64}Cu-**[2]** is higher than that from ^{64}Cu-**[1]**, even though more ^{64}Cu-**[1]** is transported to

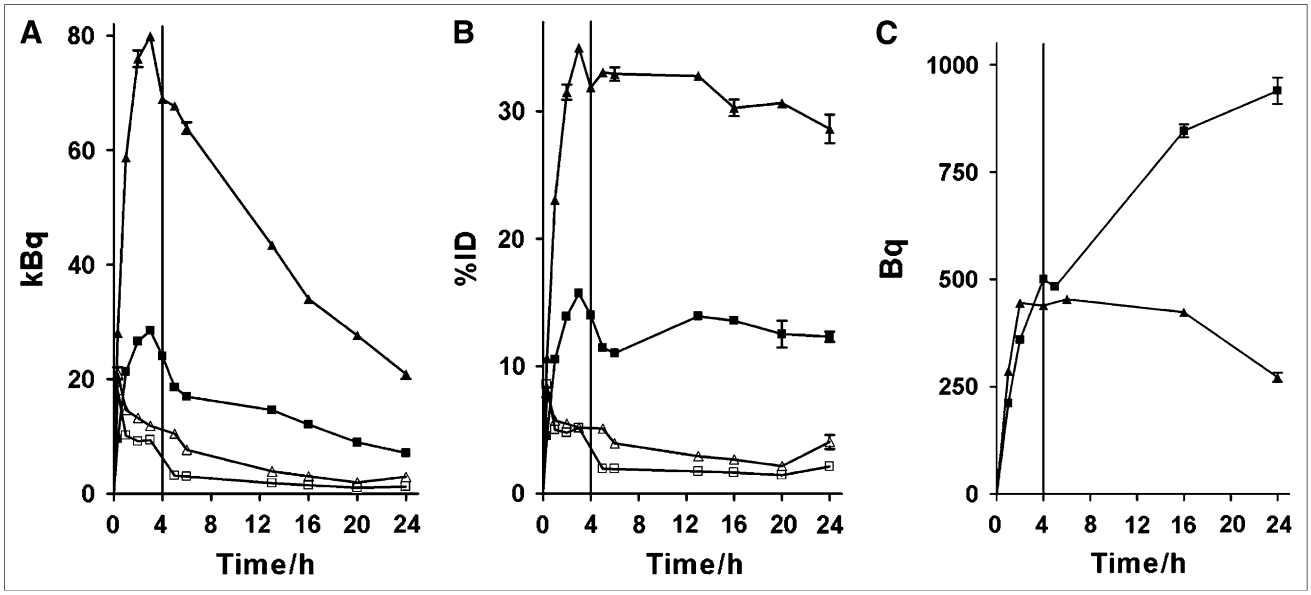

FIGURE 3. Internalization and efflux profiles of ^{64}Cu-TETA-Y3-TATE (■, internalized; □, surface-bound) and ^{64}Cu-CB-TE2A-Y3-TATE (▲, internalized; △, surface-bound) in A427-7 cells shown in kilobecquerels (A) and in %ID (B). ^{64}Cu activity in becquerels derived from ^{64}Cu-TETA-Y3-TATE (■) and ^{64}Cu-CB-TE2A-Y3-TATE (▲) localized to nuclei of A427-7 cells is shown in C. Vertical line at 4 h in A–C delineates change to fresh medium.

A427-7 cell nuclei. This stems from the substantial contribution of cytosolic activity to the nuclear dose (more ^{64}Cu-**[2]** is internalized; Fig. 3) and from the fact that ^{64}Cu from ^{64}Cu-**[1]** appears in the nucleus only later in the time course.

External Beam Irradiation

The A427-7 cells had a plating efficiency of ~22%. After exposure to various doses of x-rays, a colony-forming assay was performed and the data were fit using the linear-quadratic model for cell survival (Fig. 4B). These data show that the α/β ratio (the dose at which the linear and quadratic components of radiation damage are equal) for A427-7 cells was 2.5 and the D_{10} (the dose required to kill 90% of the cells) was 5.6 Gy. The low α/β ratio and the high D_{10} indicate that this cell line is relatively radioresistant.

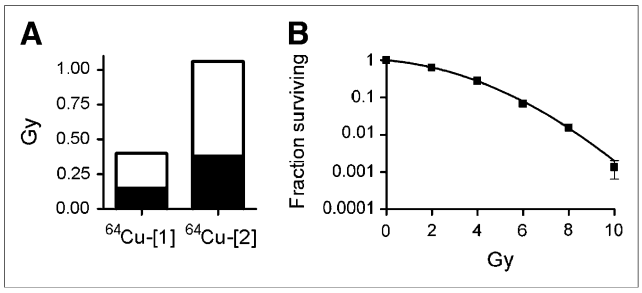

FIGURE 4. Dosimetry and cell killing by ionizing radiation. (A) Absorbed dose to A-427-7 cells from ^{64}Cu-**[1]** and ^{64}Cu-**[2]** during internalization/efflux period; dose to nucleus is indicated in black. (B) A-427-7 cells were exposed to ionizing radiation in an external beam experiment. Absorbed doses higher than 1 Gy are necessary for substantial cell killing.

DISCUSSION

When designing a radiopharmaceutical for peptide receptor radiotherapy, one of the goals is to maximize damage to the tumor cells. Irradiating the DNA is an effective way to injure and eventually kill cells; thus, a radionuclide that localizes to the cell nucleus of a tumor cell potentially enhances the efficacy of the radiopharmaceutical. This may be especially true for radionuclides whose ranges in tissues are short. ^{64}Cu decays through β^+ emission (0.655 MeV, 17.4%), β^- emission (0.573 MeV, 41%), and electron capture (0.33 MeV, 0.6%, and 1.68 MeV, 40.5%). There are 2 Auger electrons emitted per decay (840 eV and 6.8 keV), and because of the very restricted range of these low-energy electrons in biologic tissues, nuclear localization of ^{64}Cu could increase the probability of cell killing from DNA damage. Thus far, chelators have been optimized for high stability to increase uptake in target organs and avoid accumulation of the radiometal in nontarget tissues. However, for targeted radiotherapy with $^{64/67}$Cu-labeled tumor-targeting peptides or mAbs, the use of a chelator that complexes ^{64}Cu less stably after uptake into the cell could indeed prove to be more efficacious than using a chelator that complexes the copper radionuclide more stably.

We previously demonstrated that ^{64}Cu from ^{64}Cu-TETA-octreotide localizes to the nucleus of AR42J rat pancreatic tumor cells and hypothesized that dissociation of the radiometal from the chelator is the first step in this process.

Here, we compare two ^{64}Cu radiopharmaceuticals, ^{64}Cu-TETA-Y3-TATE (^{64}Cu-**[1]**) and ^{64}Cu-CB-TE2A-Y3-TATE (^{64}Cu-**[2]**). Y3-TATE–based radiopharmaceuticals are highly specific for SSTr2, have a higher affinity (typically, $IC_{50} < 2$ nM (*19*)), and are more rapidly internalized into cells expressing this receptor than octreotide-based analogs (*6*,*20*). ^{64}Cu-**[1]** demonstrated higher uptake into tumor and other somatostatin–receptor-rich tissues than ^{64}Cu-TETA-octreotide in CA20948 tumor-bearing rats and AR42J tumor-bearing severe combined immunodeficiency (SCID) mice (*21*). We subsequently demonstrated that ^{64}Cu-**[2]** showed lower nonspecific uptake in blood and liver and greater tumor uptake compared with ^{64}Cu-**[1]** (*17*).

We investigated the binding characteristics of ^{64}Cu-**[1]** and ^{64}Cu-**[2]** to somatostatin receptors on A427 non–small cell lung carcinoma cells. Several clones of this human tumor cell line are available, stably transfected with and expressing various levels of SSTr2 on the cell surface, without expression of any other somatostatin receptor subtype (*16*). The IC_{50} values compare well with those of related somatostatin analogs (*19*). Here we show an approximately 2-fold increase in SSTr2 density on A427-7 cells (B_{max}) for ^{64}Cu-**[2]** compared with that of ^{64}Cu-**[1]**, whereas we observed a 10-fold higher B_{max} value for ^{64}Cu-**[2]** compared with that of ^{64}Cu-**[1]** in AR42J cells (*17*). As AR42J cells express SSTr1, SSTr2, SSTr3, and SSTr5, differences in binding affinities to somatostatin receptor subtypes other than SSTr2 were hypothesized to explain the observed maximum receptor densities, as the assay cannot distinguish between binding to the various subtypes. A427-7 cells only express SSTr2, so here the confounding influence of other receptor subtypes cannot account for the higher B_{max} observed for ^{64}Cu-**[2]**, although the difference is not as pronounced in the AR42J cells. The Cu-CB-TE2A moiety of ^{64}Cu-**[2]** has a charge of +1, whereas the Cu-TETA moiety of ^{64}Cu-**[1]** is negatively charged due to the presence of 2 extra carboxylic acid groups. This change from a positive to a negative charge on the chelator could have an effect on the binding of the Y3-TATE peptide moiety to the somatostatin receptor, although the K_d was not significantly affected.

^{64}Cu-**[1]** and ^{64}Cu-**[2]** differ substantially with respect to the in vivo stability of the ^{64}Cu-chelate, and this has important consequences for the translocation of copper from these compounds to the cell nucleus. The half-life of Cu(II)-CB-TE2A in 5N HCl at 90°C is 154 h, whereas Cu(II)-TETA has a half-life of <5 min (*22*). In rat liver metabolism studies in vivo, ^{64}Cu from ^{64}Cu-TETA was found to dissociate and to bind to proteins (e.g., superoxide dismutase) at much higher levels than from ^{64}Cu-CB-TE2A (*23*). Our experimental results with A427-7 cells confirm this stability pattern. In A427-7 cells incubated with ^{64}Cu-**[2]**, there was only minimal ^{64}Cu localization in the nuclear fraction over a 24-h time course, whereas incubation with ^{64}Cu-**[1]** led to a 6-fold increase over the same time period. We hypothesized that dissociation of ^{64}Cu from the chelator must occur before localizing to the nucleus. Our hypothesis does not take into account the fate of the peptide portion of the radiopharmaceutical within cells, which may be subject to degradation during the internalization pathway—for example, by lysosomal processes. Other researchers have proposed the transport of intact somatostatin radiopharmaceuticals to the nucleus (*24*), although we demonstrated that the amount of ^{111}In-DTPA-octreotide delivered to AR42J cell nuclei is very small (~5% of CAA) (*15*).

The percentages of ^{64}Cu from ^{64}Cu-TETA-Y3-TATE that localized to the A427-7 nuclei at 4 and 24 h (1.3% ± 0.1% and 9.4% ± 1.7%, respectively) were substantially lower than those observed for ^{64}Cu-TETA-octreotide in AR42J cells at the same time points (10% and 20%, respectively) (*15*). This is not likely due to the use of octreotide versus Y3-TATE, as all nuclear uptake values were normalized to the percentage of agent that was cell-associated. Additionally, the same chelator (TETA) was used for both sets of experiments.

Dosimetry estimates were obtained from the uptake and efflux data (Fig. 3) for ^{64}Cu-**[1]** and ^{64}Cu-**[2]** in A427-7 cells. The results (Fig. 4A) show that even with high specific activities of ^{64}Cu-**[1]** and ^{64}Cu-**[2]**, we were not able to deliver more than 1 Gy to A427-7 cells. Treatment of the cells with external beam irradiation (Fig. 4B) at 1 Gy of radiation dose killed <20% of the cells. A study that used another somatostatin analog (DOTATOC), labeled with the β-emitter ^{177}Lu, achieved approximately 65% cell killing of Capan-2 cells at a dose of 1.53 Gy (*25*). However, this effect can be attributed only partially to somatostatin receptor-mediated internalization of ^{177}Lu-DOTATOC, because the radiolabeled chelator ^{177}Lu-DOTA itself also caused 53% cell killing of Capan-2 cells at a dose of 1.25 Gy (*25*). Our experiments with internalized ^{64}Cu-labeled somatostatin analogs show that a low dose was delivered to A427-7 cells, in part because of their large size (diameter = 19 μm). Additionally, the transport to the A427-7 nuclei of ^{64}Cu from TETA-Y3-TATE did not contribute significantly to the dose to the tumor cell nuclei, most likely because the nuclear localization did not increase substantially until the 24-h time point, unlike in AR42J cells, where transport to the nucleus occurred as early as 4 h (*15*). For these reasons, we chose not to pursue cell-killing experiments in A427-7 cells.

CONCLUSION

The data presented here support our hypothesis that the mechanism of ^{64}Cu delivery to the nuclei of tumor cells by ^{64}Cu-labeled somatostatin analogs after internalization involves dissociation from the chelator followed by translocation to the nucleus. A highly stable ^{64}Cu-CB-TE2A-Y3-TATE (^{64}Cu-**[2]**) showed very low amounts of nuclear localization compared with the less-stable ^{64}Cu-TETA-Y3-TATE (^{64}Cu-**[1]**). High levels of internalization were obtained with both compounds; however, only <1 Gy of

radiation dose was delivered by either ^{64}Cu-labeled somatostatin analog.

ACKNOWLEDGMENTS

The authors gratefully acknowledge Susan Adams for technical support and Jesse Parry for technical assistance and helpful discussions. Funding was provided by National Cancer Institute grants 5 R01 CA064475 and R24 CA86307 (production of ^{64}Cu at Washington University School of Medicine), and National Institute of Biomedical Imaging and Bioengineering grant R01 EB 004533.

REFERENCES

1. Krenning EP, Kwekkeboom DJ, Bakker WH, et al. Somatostatin receptor scintigraphy with [^{111}In-DTPA-D-Phe^{1}]- and [^{123}I-Tyr^{3}]-octreotide: the Rotterdam experience with more than 1000 patients. *Eur J Nucl Med.* 1993;20:716–731.
2. Krenning EP, Kooij PPM, Pauwels S, et al. Somatostatin receptor: scintigraphy and radionuclide therapy. *Digestion.* 1996;57(suppl. 1):57–61.
3. de Jong M, Breeman WAP, Bakker WH, et al. Comparison of ^{111}In-labeled somatostatin analogues for tumor scintigraphy and radionuclide therapy. *Cancer Res.* 1998;58:437–441.
4. Stolz B, Weckbecker G, Smith-Jones PM, Albert R, Raulf F, Bruns C. The somatostatin receptor-targeted radiotherapeutic [^{90}Y-DOTA-DPhe^{1},Tyr^{3}]octreotide (^{90}Y-SMT 487) eradicates experimental rat pancreatic CA 20948 tumours. *Eur J Nucl Med.* 1998;25:668–674.
5. de Jong M, Breeman WAP, Bernard BF, et al. [^{177}Lu-DOTA^{0}-Tyr^{3}]octreotate for somatostatin receptor-targeted radionuclide therapy. *Int J Cancer.* 2001;92:628–633.
6. Anderson CJ, Jones LA, Bass LA, et al. Radiotherapy, toxicity and dosimetry of copper-64-TETA-octreotide in tumor-bearing rats. *J Nucl Med.* 1998;39: 1944–1951.
7. Lewis JS, Lewis MR, Cutler PD, et al. Radiotherapy and dosimetry of ^{64}Cu-TETA-Tyr3-octreotate in a somatostatin receptor-positive tumor-bearing rat model. *Clin Cancer Res.* 1999;5:3608–3616.
8. Bushnell D, Menda Y, Madsen M, et al. Assessment of hepatic toxicity from treatment with ^{90}Y-SMT 487 (OctreoTher™) in patients with diffuse somatostatin receptor positive liver metastases. *Cancer Biother Radiopharm.* 2003;18:581–588.
9. de Jong M, Breeman WA, Valkema R, Bernard BF, Krenning EP. Combination radionuclide therapy using ^{177}Lu- and ^{90}Y-labeled somatostatin analogs. *J Nucl Med.* 2005;46(suppl 1):13S–17S.
10. Pless M, Waldherr C, Maecke H, Buitrago C, Herrmann R, Mueller-Brand J. Targeted radiotherapy for small cell lung cancer using 90yttrium-DOTATOC, an yttrium-labelled somatostatin analogue: a pilot trial. *Lung Cancer.* 2004;45:365–371.
11. Kwekkeboom DJ, Bakker WH, Kam BL, et al. Treatment of patients with gastro-entero-pancreatic (GEP) tumours with the novel radiolabelled somatostatin analogue [^{177}Lu-DOTA(0),Tyr3]octreotate. *Eur J Nucl Med Mol Imaging.* 2003; 30:417–422.
12. Froidevaux S, Eberle AN. Somatostatin analogs and radiopeptides in cancer therapy. *Biopolymers.* 2002;66:161–183.
13. Connett JM, Anderson CJ, Guo LW, et al. Radioimmunotherapy with a Cu-64-labeled monoclonal antibody: a comparision with Cu-67. *Proc Natl Acad Sci USA.* 1996;93:6814–6818.
14. Connett JM, Buettner TL, Anderson CJ. Maximum tolerated dose and large tumor radioimmunotherapy studies of ^{64}Cu-labeled MAb 1A3 in a colon cancer model. *Clin Cancer Res.* 1999;5:3207s–3212s.
15. Wang M, Caruano AL, Lewis MR, Meyer LA, VanderWaal RP, Anderson CJ. Subcellular localization of radiolabeled somatostatin analogues: implications for targeted radiotherapy of cancer. *Cancer Res.* 2003;63:6864–6869.
16. Parry JJ, Eiblmaier M, Andrews R, et al. Characterization of somatostatin receptor subtype 2 expression in stably transfected A-427 human cancer cells. *Mol Imaging.* 2007;6:56–67.
17. Sprague JE, Peng Y, Sun X, et al. Preparation and biological evaluation of copper-64-Tyr^{3}-octreotate using a cross-bridged macrocyclic chelator. *Clin Cancer Res.* 2004;10:8674–8682.
18. Goddu SM, Howell RW, Bouchet LG, Bolch WE, Rao DV. *MIRD Cellular S Values: Self-Absorbed Dose per Unit Cumulated Activity for Selected Radionuclides and Monoenergetic Electron and Alpha Particle Emitters Incorporated into Different Cell Compartments*. New York, NY: Society of Nuclear Medicine; 1997.
19. Reubi JC, Schar J-C, Waser B, et al. Affinity profiles for human somatostatin receptor subtypes SST1-SST5 of somatostatin radiotracers selected for scintigraphic and radiotherapeutic use. *Eur J Nucl Med.* 2000;27:273–282.
20. Lewis JS, Lewis MR, Srinivasan A, Schmidt MA, Wang J, Anderson CJ. Comparison of four ^{64}Cu-labeled somatostatin analogs *in vitro* and in a tumor-bearing rat model: evaluation of new derivatives for PET imaging and targeted radiotherapy. *J Med Chem.* 1999;42:1341–1347.
21. Lewis JS, Srinivasan A, Schmidt MA, Anderson CJ. In vitro and in vivo evaluation of ^{64}Cu-TETA-Tyr^{3}-octreotate: a new somatostatin analog with improved target tissue uptake. *Nucl Med Biol.* 1999;26:267–273.
22. Woodin KS, Heroux KJ, Boswell CA, et al. Kinetic inertness and electrochemical behavior of Cu(II) tetraazamacrocyclic complexes: possible implications for in vivo stability. *Eur J Inorg Chem.* 2005;4829–4833.
23. Boswell CA, Sun X, Niu W, et al. Comparative *in vivo* stability of copper-64-labeled cross-bridged and conventional tetraazamacrocyclic complexes. *J Med Chem.* 2004;47:1465–1474.
24. Hornick CA, Anthony CT, Hughey S, Gebhardt BM, Espenan GD, Woltering EA. Progressive nuclear translocation of somatostatin analogs. *J Nucl Med.* 2000;41:1256–1263.
25. Nayak T, Norenberg J, Anderson T, Atcher R. A comparison of high- versus low-linear energy transfer somatostatin receptor targeted radionuclide therapy in vitro. *Cancer Biother Radiopharm.* 2005;20:52–57.

JNM The Journal of NUCLEAR MEDICINE

Nuclear Uptake and Dosimetry of ^{64}Cu-Labeled Chelator–Somatostatin Conjugates in an SSTr2-Transfected Human Tumor Cell Line

Martin Eiblmaier, Rebecca Andrews, Richard Laforest, Buck E. Rogers and Carolyn J. Anderson

J Nucl Med. 2007;48:1390-1396.
Published online: July 13, 2007.
Doi: 10.2967/jnumed.107.039990

The Journal of Nuclear Medicine is published monthly.
SNMMI | Society of Nuclear Medicine and Molecular Imaging
1850 Samuel Morse Drive, Reston, VA 20190.
(Print ISSN: 0161-5505, Online ISSN: 2159-662X)

SNMMI SOCIETY OF NUCLEAR MEDICINE AND MOLECULAR IMAGING